University of North Carolina Asheville
Journal of Undergraduate Research
Asheville, North Carolina
May 2019

Study of Temperature and Mineralizer Effects on the Hydrothermal Synthesis of Titanium Dioxide Nanoparticles

Joshua Davis
Chemistry Department
The University of North Carolina at Asheville
One University Heights
Asheville, North Carolina 28804 USA

Faculty Advisor: Dr. Oksana Love

Abstract

Nanoparticulate photocatalysts are a highly studied topic in the field of heterogeneous catalysis. In particular, titanium dioxide nanoparticles are considered a promising candidate for many photocatalytic and photoelectric applications. However, the size, surface structure, and crystalline morphological control of these particles is a pressing issue in the field due to the electronic structures dependence on these properties. This project analyzes the optimal synthetic conditions to generate brookite phase nanoparticles using the hydrothermal method. This project also analyzes the utilization of mineralizers to control for surface structure and particle size. The particles crystalline shape and surface structure were analyzed using powder X-ray Diffraction and Scanning Electron Microscopy. Overall, a repeatable hydrothermal method with a mono dispersion of size and control on surface structure was developed. Also in terms of mineralizer utilization, it appears that higher concentrations of mineralizer gave rise to similar morphologies as the control while lower mineralizer concentrations generated a wider variety of surface structures and sizes.

1. Introduction

In 1856 Michael Faraday proposed the concept of a new type of structure larger than individual atoms though smaller than microscopic particle after his discovery of a gold nanoparticle colloid. Faraday had just discovered a new particle size of structured matter: the nanoparticle.[1] Nanoparticles (NPs) are structures that have dimensions on the scale of 10^{-9} meters and are known for having a large surface area to mass ratio. Since chemical reactions involving solids are largely dependent on the shape and area of the surface, NPs are generally favored as the materials for catalytic applications.[2] In particular, there is a large field of interest in the photocatalytic applications of nanoparticle catalysts.[3-6] This is due to the near visible band gap with a highly tunable and size dependent position in the electromagnetic spectrum.[7-8]

In 1972, Fujishima *et. al.* discovered that titanium dioxide, TiO_2, electrodes were able to split water when irradiated with light. After that, TiO_2 has been actively studied for its photocatalytic properties and photovoltaic applications.[9] TiO_2, like many other metal chalcogenides, have three different crystalline structures: anatase, rutile, and brookite. The majority of work done in the field of TiO_2 photocatalysis has been on the anatase and rutile forms. This is because the majority of processes for forming TiO_2 create the anatase and rutile morphologies as the main products while the brookite morphology is generated as a side product.[10] It is suggested that brookite is unstable due the low structural symmetry in its orthorhombic crystal system, unlike the tetragonal system in the anatase and rutile.[11] Anatase is constructed of edge sharing TiO_6 octahedra while rutile is composed of total corner sharing octahedra. However, brookite is comprised of a mixture of edge sharing and corner sharing octahedra, which in turn creates a less symmetric crystal system, making brookite a less stable and harder to synthesize.[12]

Since TiO_2 is a solid state heterogeneous catalyst, all photocatalytic reactions must happen at the surface of the material. Through the formation of NPs, the material has a large surface area and reacts more with pollutants. From previous literature, it has been proposed that the surface construction of these NPs is the ultimate factor in determining

the reactivity of a nanoparticle in catalysis.[13-15] However, all of this work has been done on the anatase and rutile phases of TiO_2 with little research currently being done on these effects in brookite structures. In particular, tuning the surface construction of brookite TiO_2 NPs to manipulate reactivity.[16]

In Richeng Yu's research group, extensive work is being done on the tuning of metal oxide catalysts reactivity by varying the facets exposed on the surface of TiO_2 NPs. The facets are the crystallographic planes present on the surface of the nanoparticles. The group synthesized three different particle shapes of TiO_2 NPs with varying ratios of lateral facets to determine their effects on the catalytic activity of the surfaces. They also discovered that highly irregular surfaces such as nanospindles and nanoflowers had lower reactivity in photocatalytic reactions. This meant that the highly irregular surfaces were inert compared to the flat surfaces due to increased charge recombination.[13] Furthermore, the group performed a literature review on the tailoring of TiO_2 crystals with specific facets to tune properties of materials in which they concluded that there is a large variety of methods used to tune crystals to favor certain facets; such as, pH, temperature, concentration, and solvation conditions along with many others.[17]

Sun's group reported the synthesis of brookite TiO_2 fractal structures called "flowers". The group utilized a hydrothermal method for synthesizing these nanostructures. The crystallization mechanism described by the group begins with the nucleation of small seed crystals formed in a solution which are then subsequently elongated into larger crystals which are structurally stabilized by the sodium and hydroxide ions present in the solution. This growth process continues until Ostwald ripening is observed in the system. After the crystals reach a certain size, the attraction between different surfaces overcome the stabilizing charges of the sodium and hydroxide ions in the solution cause the nanoflower agglomerates to form.[18-20]

When looking at the effects the non-participating ions, such as the sodium or hydroxide ions, have on the hydrothermal process, previous literature has discussed the utilization of mineralizers.[17] A mineralizer is an additive which acts as a catalyst for seed formation and selector for different surface structures of crystals. This phenomena happens through surface charge minimization and the alteration of solubility conditions for crystalline precursors.[21] Previous groups have utilized mineralizers to select for optimal sizes and shapes of varying nanostructures such as $Cd(OH)_2$, ZnO, $BiFeO_3$, and Zn_2SnO_4 nanostructures for electronic applications.[21-24] These groups have shown the possibility of controlling surface structure and in turn the electronic band structure of nanoparticles through the use of these mineralizer assisted methods.

The overall goal of this project was to develop a reproducible method for controlling the surface structure and particle size of brookite titanium dioxide at pH of 12.5. To do this, the project was divided into three phases. The first phase was to determine the optimal temperature and time parameters of the hydrothermal synthesis adapted from the procedures described previously. The second phase consists of utilizing sodium chloride as an alkali metal salt mineralizers to control the surface structure and particle shape of the TiO_2 NPs. During this phase, the concentration of sodium chloride was changed to determine whether the change in solvation conditions would generate different nanoparticle structures through the selection of varying surface structures.

2. Experimental Methods

The procedure used in this project is adapted from the hydrothermal synthesis previously reported in the literature.[6] All sample syntheses were done in aqueous solution and all hydrothermal crystallizations were done in a Teflon-lined stainless steel autoclave.

For each synthesis, a 100 mL 0.31 M solution of titanium oxysulfate ($TiOSO_4$) was created and a stock solution of 0.21 M sodium hydroxide (NaOH) was made. For each synthesis 100 mL of 0.21 M NaOH solution was added to the 100mL 0.31 M $TiOSO_4$ solution. After reacting for 30 min under ambient conditions, a milky white gel precipitated from solution. The suspension was then washed through centrifugation at 5000 rpm for 5 minutes and sonication for 5 minutes, repeated three times. After decanting the supernatant solution, the white solid was then suspended in 50 mL of deionized water. Next, concentrated sodium hydroxide was added to raise the pH of the suspension to 12.5. The solution was then transferred into a 75 mL Teflon-lined stainless steel autoclave and was heated, in an air convection oven, at different times ranging from 48 hours to 72 hours and at a range of different temperatures ranging from 200 °C to 220 °C. The range of temperatures and times used in the synthesis can be seen in **Table 1.**

Table 1. List of all reaction parameters for each sample

Temperature	Time	Sample
200 °C	48 hours	A
200 °C	72 hours	B
220 °C	48 hours	C
220 °C	72 hours	D

After reacting in the autoclave, the colloid was centrifuged at 3500 rpm for 10 minutes and sonicated for five minutes, this process was performed at least 4 times or until the supernatant was clear. All NP samples were characterized using Powder X-ray Diffraction, X'Pert PRO Diffractometer, to determine crystal structure. Then they were characterized with Scanning Electron Microscopy using an FEI Quanta 400.

Upon further investigation of the role mineralizer had in the hydrothermal synthesis, the concentration of mineralizer was varied to determine the correlation between crystalline structure and NaCl concentration. For each synthesis all samples were made using the procedures outlined during the time and temperature optimization. The only variation was during the process of loading the sample into the autoclave, mineralizer at varying concentrations (listed below) were added to the container before sealing.

All samples were then analyzed using Powder X-ray Diffraction, X'Pert PRO Diffractometer, to determine crystal structure. Then they were characterized using Scanning Electron Microscopy using an FEI Quanta 400.

Table 2. List of different concentrations of NaCl comparative moles to $TiOSO_4$.

Sample	NaCl : $TiOSO_4$ Molar Ratio
M1	1:1 (100%)
M2	0.5:1 (50%)
M3	0.1:1 (10%)
M4	1:1.4 (71%)

3. Results and Discussion

3.1 Time and Temperature Control Experiment

To determine the crystal structure of the NPs the diffractograms of each sample was compared to pre-purchased anatase, rutile, and brookite standards. **Figure 1** shows a comparison of the P-XRD data between the synthesized brookite NPs and the purchased anatase, rutile, and brookite NPs. By comparing the diffractogram of anatase from previous literature to the standard TiO_2, the crystalline facets (or crystalline planes) can be identified as:(101) at angle 2Θ=25.23, (004) at angle 2Θ=37.72, and (211) at angle 2Θ= 53.77 found using Bragg's Law and defined d spacings.[26] The brookite phase standard was compared to previous literature and the facets were identified as: (111) at angle 2Θ=25.73, (211) at angle 2Θ=30.84, (121) at angle 2Θ=38.63, (202) at angle 2Θ=40.18, (221) at angle 2Θ=42.36, (321) at angle 2Θ=48.04, (122) at angle 2Θ=49.73, (113) at angle 2Θ=57.16, (231) at angle 2Θ=57.35.[26] The rutile

phase standard was not annotated due to lack of peak overlap with any synthesized samples. Sample **A** was identified as an anatase phase crystalline structure due to the matching peaks with anatase. Samples B and C were identified as brookite phase due to the matching peaks with brookite standard. Sample D was identified as brookite morphology; however, the product was partially amorphous due to the undefined (113), (231) and (321) facets.

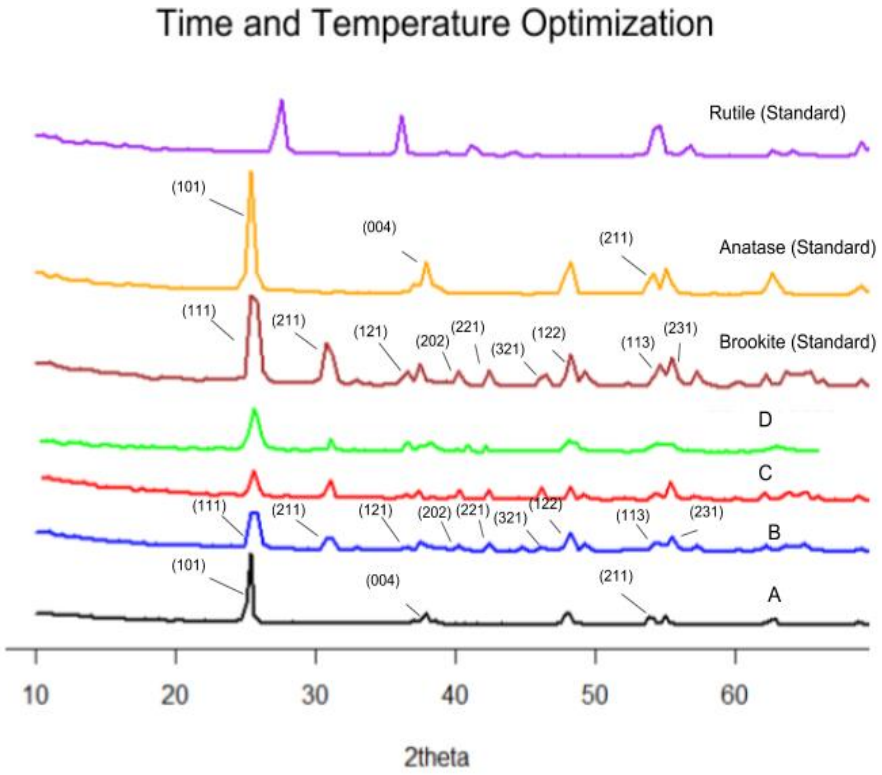

Figure 1. Powder X-ray diffractograms of Anatase, Brookite, and Rutile standards along with NPs synthesized at 200 °C for 48 hrs (A), 200 °C for 72 hrs (B), 220 °C for 48 hrs (C), 220 °C for 72 hrs (D).

The P-XRD data confirmed as the diffractograms for **B** and **C** match that of the pre-bought brookite standard. However, synthesis **A** matched that of the anatase standard; therefore, the synthesis at 200 °C for 48 hrs was unable to reach the preferred reaction conditions required to produce a brookite phase nanostructure. It is theorized that synthesis **D** was heated at too high of a temperature, 220 °C, for too long, 72 hrs. Though these reactions conditions created brookite phase nanoparticles, the product was less crystalline than sample **B** and **C**.

Figure 2 shows SEM images that were taken of the nanoparticle samples A, B, C, and D. When the images are compared, it is clear that a more defined particle shape can be seen at higher temperatures and longer times. As seen in the sample **C** SEM image, the NPs have an oblong shape. This can also be seen slightly in the sample **B** SEM image. However, samples **A** and **D** seem to have no defined shape of clear NPs. A higher resolution microscopy method would be required to further analyze the shape of the NPs. A clear progression of increase in crystal size can be seen with longer reaction times; though, reaction times proceeding for too long have caused the NPs to enter into another phase.

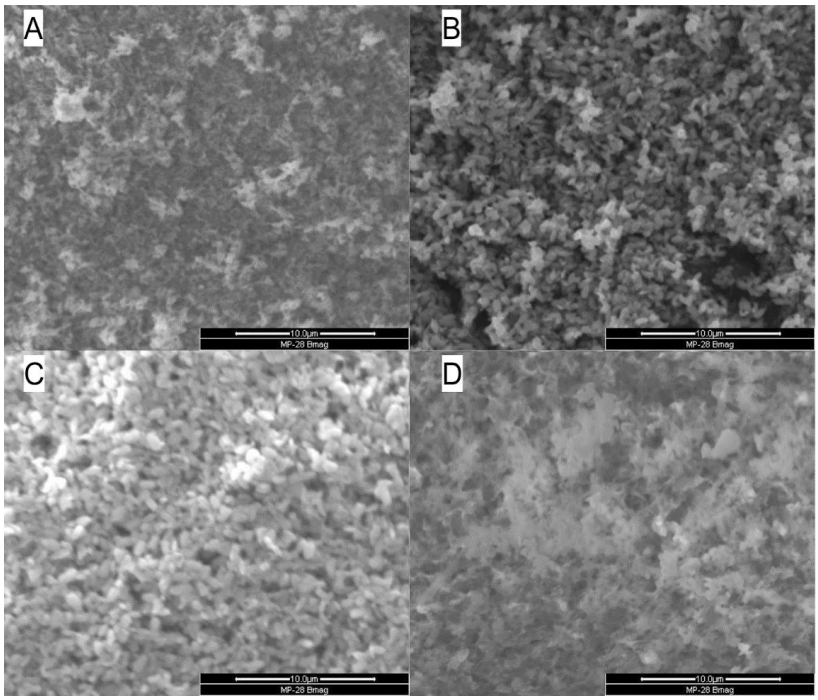

Figure 2. Scanning Electron Microscopy image of pre-bought brookite NPs (top left), brookite NPs synthesized at 200 °C for 48 hrs (top right), synthesized at 220 °C for 48 hrs (bottom left), and 220 °C for 96 hrs (bottom right).

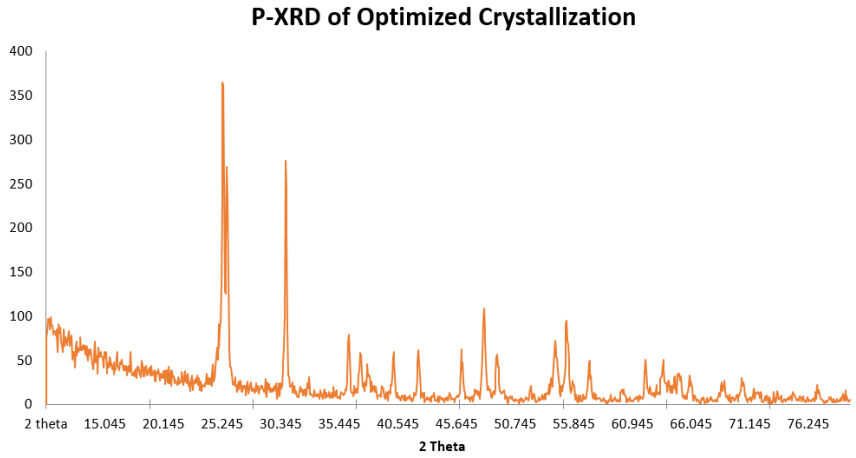

Figure 3. Powder X-ray diffractogram of optimized NP synthesis with condition of 220°C and 48 hrs

When analyzing both the crystalline structure and NP shape and size, an optimized synthetic procedure was generated. In this method, the nanoparticles were heated at 220°C for 48 hrs to generate large, monodispersed NPs as seen in **Figure 4**. Moreover, the crystalline structure of the product was highly crystalline and aligned closely with the peaks indicative of a pure brookite crystalline phase which can be seen in **Figure 3**. While the size was in the microscale on a range of 1µm, the shape was still mostly homogenous being "hop-like" in surface structure and the crystal structure was correlated exactly with that of the brookite state. The development of this optimized synthesis was the basis of the mineralizer based experiments and was used for all syntheses.

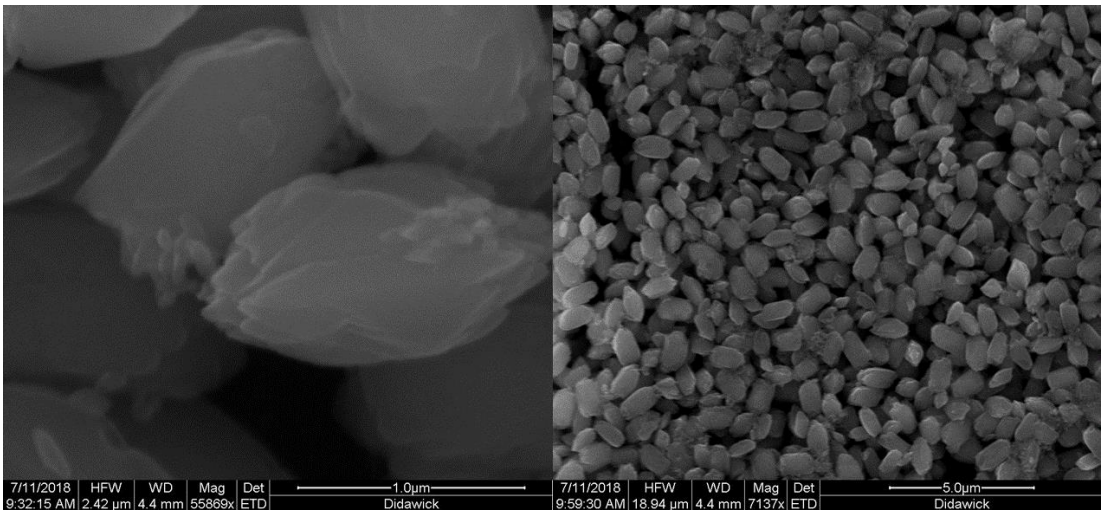

Figure 4. Nanoparticles synthesized under optimal conditions (220°C, 48 hrs) at 1µm (left) and 5µm (right)

3.2 Mineralizer Concentration Variation Experiment

In order to identify the crystalline structure, Powder X-ray diffraction was performed on products generated at different NaCl concentrations (0.1:1, 0.5:1, 1:1, and 1:1.4) and their corresponding controls. As seen in **Figure 5** the crystalline structure of all controls was brookite in morphology. This can be seen with the peaks present at 2Θ=25.73, 2Θ=30.84, 2Θ=40.18, 2Θ=57.16, and 2Θ=57.35 degrees signifying the presence of the (111), (211), (202), (113), and (231) facets respectively. It is important to note that both the M1 (1:1) concentration, (M4) concentration and all controls had the same peak at 2Θ=32.8 which was defined in previous literature. However, in samples M2 and M3 this peak appears to be absent suggesting that at lower NaCl concentrations that facet is absent. This phenomenon could be due to either the selection of a facet or due to decreased crystallinity. In general, it is apparent that while the crystallinity of each sample was varied, the overall brookite morphology stayed the same.

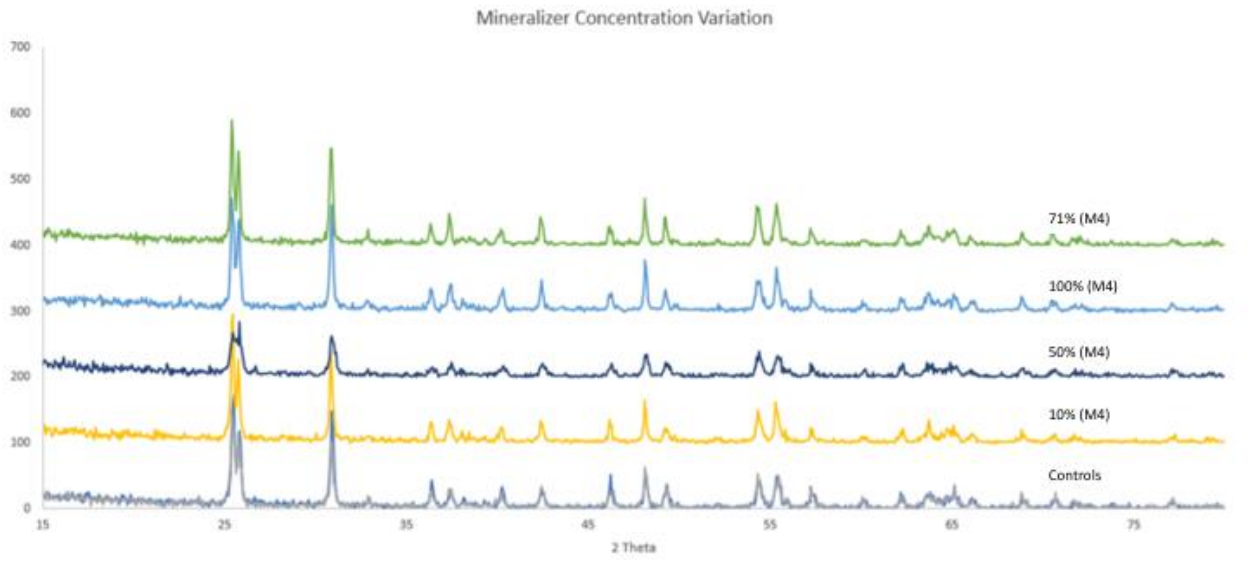

Figure 5. Comparison of controls (bottom), 100% NaCl:$TiOSO_4$ (M1), 50% (M2), 10% (M3), and 71% (M4)

Scanning electron micrographs were taken of the products synthesized at concentrations of 1:1 (M1), 0.5:1 (M2), 0.1:1 (M3), and 1:1.4 (M4) along with their corresponding controls. As seen in **Figure 6**, the 1:1 molar ratio of

mineralizer to titanium oxysulfate (A) generates a parallelepiped or rhomboid structure and NPs roughly 500 nm size. The 1:1.4 ratio (D) was similar in shape and size to the 1:1 ratio proving similar structural moieties were present. It is important to note that both samples M1 and M4 were monodispersed in size showing control over size at high concentrations. The 0.5:1 mineralizer ratio (B) appears to be less homogenous in size and shape with a range from 100nm to 1µm in length and wide variety of shapes. The same can be said for the 0.1:1 mineralizer ratio (C) with little homogeneity in shape and a large variation in size ranging from <100nm to >500nm in length. All samples M1-M4 while brookite in crystalline structure were smaller in size (roughly 100-500nm) to the control (roughly 1 µm). These samples also had a different surface morphology than the control with M1 and M4 being a monodispersed rhomboid shape while M2 and M3 varied greatly.

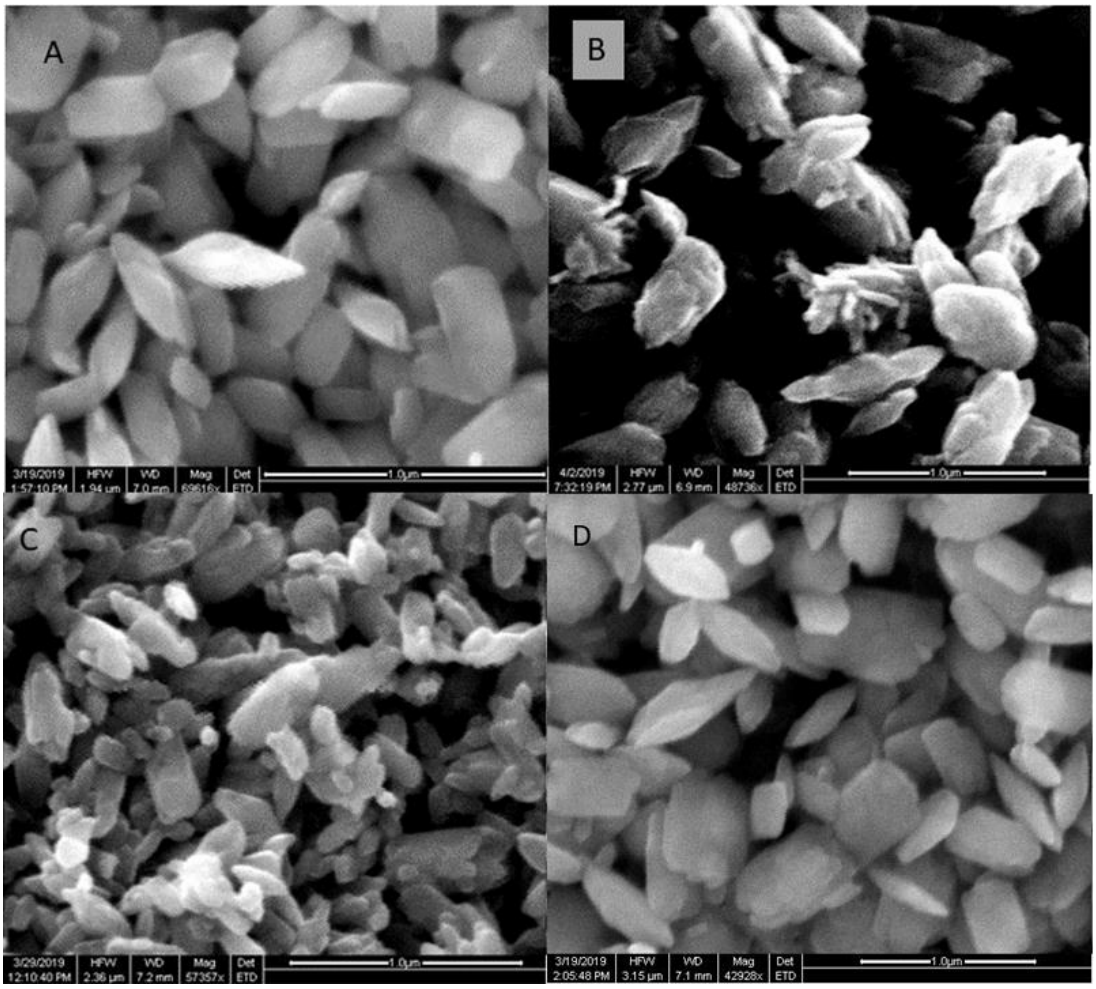

Figure 6 TiO_2 NPs made using a 100% NaCl:$TiOSO_4$ ratio (top left), 50% ratio (top right), a 10% ratio (bottom left), and 71% ratio (bottom right)

With respect to the variation in mineralizer concentration, it is apparent that the generation of multiple NPs structures and sizes occurs at lower concentrations, such as 0.1:1 and 0.5:1. While at higher concentrations, such as 1:1 and 1:1.4, the NPs appear to have a sustained rhomboidal shape and approximately 500 nm in length. In terms of shape and size control, it appears that the mineralizer is effective at preventing growth up to or past the 1 µm range keeping the nanoparticles mesoscale in size. One explanation for this effect could be that the presence of sodium chloride in the solution prevents Ostwald ripening from occurring due to a lower surface energy on the particles induced by stabilization through sodium and chloride ions. These phenomena would also explain the lack of "hop-like" surface structure present in the mineralizer samples due to little or no particle agglomeration. However, the crystallinity of the nanoparticles appears to be limited at lower concentration and more defined at higher concentrations. Overall, the

ability to change surface structure and particle size while maintaining a brookite morphology was demonstrated through the use of varying mineralizer concentrations.

4. Conclusion

The development of a robust hydrothermal synthesis of TiO_2 with control over surface structure and particle size using alkali metal salt mineralizers was the main focus of this project. Overall the optimal time and temperature parameters were determined for this synthetic technique at 220 °C and 24 hr. A deeper understanding of the mineralizer to titanium precursor ratio was developed using a concentration dependent study. This investigation proved in concept that the utilization of sodium chloride mineralizers is an effective way to change nanoparticle surface morphology and size through hydrothermal crystallization. While the concentration of mineralizer was required to be high in order to induce the selection of certain shapes; in general, it was highly effective at selecting for sizes at or above the 500nm scale in high concentrations along with a widespread array of sizes and shape at lower concentrations. Overall, variation of particle shape and size through alteration in time and temperature and then mineralizer concentration was achieved. Future work will investigated the variation of all three parameters (mineralizer concentration, time, and temperature) throughout the system to develop a more controlled method of selecting for size and shape using hydrothermal crystallization.

5. References

1. Faraday, M.; *Faradays Notebook: Gold Colloids*. London, 1832;
2. Agrios, A; Pichat, P.; State of the art and perspectives on materials and applications of photocatalysis over TiO_2 *J. Appl. Electrochem.*, **2005**, 35, 655-663.
3. Xiaolei, Q.; Alvarez, P.; Qilin, L.; Applications of nanotechnology in water and wastewater treatment. *Water Res.* **2013**, *47*, 3931-3946.
4. Bai, Y.; Mora-Sero, I; Angelis, F.; Bisquert, J.; Wang, P.; Titanium Dioxide Nanomaterials for Photovoltaic Applications *Chem. Rev.*, **2014**, 114,10095-10130.
5. Choi, M.; Lim, J.; Baek, M.; Choi, W.; Kim, W.; Yong, K.; Investigating the Unrevealed Photocatalytic Activity and Stability of Nanostructured Brookite TiO_2 Film as an Environmental Photocatalyst *Appl. Mater. Interfaces*, **2017**, 9, 16252−16260.
6. Chen, X.; Mao, S.; Titanium Dioxide Nanomaterials: Synthesis, Properties, Modifications, and Applications *Chem. Rev.*, **2007**, 107, 2891−2959.
7. Chen, D.; Yang, D.; Wang, Q.; Jiang, Z.; Effects of Boron Doping on Photocatalytic Activity and Microstructure of Titanium Dioxide Nanoparticles *Ind. Eng. Chem. Res*., **2006**, 45, 4110-4116.
8. Landmann, M.; Rauls E.; Schmidt, W.G.; The electronic structure and optical response of rutile, anatase and brookite TiO_2 *J. Phys.: Condens. Matter*, **2012**, 24, 195503.
9. Yun, H. J.; Lee, H.; Joo, J. B.; Kim, N. D.; Yi, J.; Effect of TiO_2 Nanoparticle Shape on Hydrogen Evolution via Water Splitting. *J. Nanosci. Nanotechnol.*, **2011**, 11, 1688-1691.
10. Paolo, A.; Bellardita, M.; Palmisano, L.; Brookite, the Least known TiO_2 Photocatalyst. *Catalysts* **2013**, *3*, 36-73.
11. Yang, Z.; Wang, B.; Cui, H.; An, H.; Pan, Y.; Zhai J.; Synthesis of Crystal-Controlled TiO_2 Nanorods by a Hydrothermal Method: Rutile and Brookite as Highly Active Photocatalysts *J. Phys. Chem. C*, **2015**, 16905-16912.
12. Dambournet, D.; Belharouak, I.; Amine, K.; Tailored Preparation Methods of TiO_2 Anatase, Rutile, Brookite: Mechanism of Formation and Electrochemical Properties. *Chem. Mat.*, **2009**, 22, 1173-1179.
13. Carp, O.; Huisman, C.L.; Reller, A.; Photoinduced reactivity of titanium dioxide. *Prog. Solid State Chem.* **2004**, *32*, 33-177.
14. Lin, H.; Li, L.; Zhao, M.; Huang, X.; Chen, X.; Li, G.; Yu, R.; Synthesis of High-Quality Brookite TiO_2 Single-Crystalline Nanosheets with Specific Facets Exposed: Tuning Catalysts from Inert to Highly Reactive. *J. Am. Chem. Soc.* **2012**, *134*, 8328-8331.
15. Liu, G.; Yang, H.; Pan, J.; Yang, Y.; Lu, G; Cheng, H.; Titanium Dioxide Crystals with Tailored Facets *Chem. Rev.* **2013**, *114*, 9559-9612.
16. Nam, Y.; Li, L.; Lee, J.; Prezhdo O.; Size and Shape Effects on Charge Recombination Dynamics of TiO_2 Nanoclusters *J. Phys. Chem. C*, **2018**, 122, 5201-5208.

17. Kim, K.; Annamalai, A.; Park, S.H.; Kwon, T.H.; Pyeon, M.W.; Lee, M.; Preparation and electrochemical properties of surface-charge-modified Zn_2SnO_4 nanoparticles as anodes for lithium-ion batteries *Electrochimica Acta*, **2012**, 76, 192–200.
18. Kandiel, T.; Feldhoff, A.; Robben ,L.; Dillert, R.; Bahnemann, D.; Tailored Titanium Dioxide Nanomaterials: Anatase Nanoparticles and Brookite Nanorods as Highly Active Photocatalysts *Chem. Mater*., **2010**, 22, 2050-2060.
19. Barnard A.S.; Curtiss, L.A.; Prediction of TiO_2 Nanoparticle Phase and Shape Transitions Controlled by Surface Chemistry *Nano Lett.*, **2005**, 5, 1261-1266.
20. Rong, A.; Gao, X.P.; Li, G.R.; Yan, T.Y.; Zhu, H.Y.; Qu, J.Q.; Song, D.Y.; Hydrothermal Synthesis of Zn_2SnO_4 as Anode Materials for Li-Ion Battery *J. Phys. Chem*. B, **2006**, 110, 14754.
21. Tang,B. ; Zhuo, L.; Ge, J.; Niu, J.; Shi, Z.; Hydrothermal Synthesis of Ultralong and Single-Crystalline $Cd(OH)_2$ Nanowires Using Alkali Salts as Mineralizers. *Inorg. Chem.*, **2005**, 44, 2568−2569.
22. Wang, Y.; Xu, G.; Ren, Z.; Wei, X.; Weng, W.; Du, P; Shen, G.; Hanw, G; Mineralizer-Assisted Hydrothermal Synthesis and Characterization of $BiFeO_3$ Nanoparticles. *J. Am. Ceram. Soc.*, **2007**, 90, 2615–2617.
23. Zhang, H.; Yang1, D.; Ma, X.; Ji, Y.; Xu, J.; Que, D.; Synthesis of flower-like ZnO nanostructures by an organic-free hydrothermal process. *Nanotechnology*, **2004**, 15, 622.
24. Hansen, J.; Sallmén, M.; Seldén,; Ahti Anttila,; Kjell, E.; Andersson, J.; Bryngelsson, I.; Raaschou-Nielsen, O.; Jørgen A.; Olsen, H.; McLaughlin, J.; Risk of Cancer Among Workers Exposed to Trichloroethylene: Analysis of Three Nordic Cohort Studies *JNCI*, **2013**, 105, 869–877.
25. Jaeger, J. W.; Carlson, I. H.; Porter, W. P.; Endocrine, immune, and behavioral effects of aldicarb (carbamate), atrazine (triazine) and nitrate (fertilizer) mixtures at groundwater concentrations. *Toxicol. Ind. Health*, 1999, 15, 133–151.
26. Downs, B.; Swaminathan, R.; Bartelmehs, K.; *American Mineralogist*, **1993** 78, 1104-1107.